



A B-Spline Interpolation Based Method for Reconstruction of Image from Partial Data

Amba D. Bhatt¹, Ujjaval Gupta², Vishal Wagholikar³, Ravi M. Warkhedkar⁴ and Amrith Thandra⁵

¹ Motilal Nehru National Institute of Technology, Allahabad, India, amba_bhatt@yahoo.com

² Motilal Nehru National Institute of Technology, Allahabad, India, ujjaval88@gmail.com

³ Motilal Nehru National Institute of Technology, Allahabad, India, vwagholikar@yahoo.in

⁴ Government College of Engineering, Aurangabad, India, raviwarkhedkar@yahoo.co.in

⁵ Motilal Nehru National Institute of Technology, Allahabad, India, amrith.thandra@gmail.com

ABSTRACT

In this paper, a method of data removal from images and then reconstruction of those images has been discussed. Images are reconstructed using B-Spline based interpolation of their Gray intensities and detailed qualitative and quantitative analysis has been carried out. The original and regenerated images are compared to generate graphical error profiles. Two techniques of B-Spline interpolation have been used. Error produced by both has been compared on the basis of parameters like mean error, standard deviation and variance. The same method is used for color data and the reconstruction results were impressive even at 2% of the original data. Apart from data-compression, this method can be used to regenerate images of good quality from low quality images and archived images which have deteriorated over time.

Keywords: image reconstruction, B-Spline, interpolation.

DOI: 10.3722/cadaps.2012.531-547

1 INTRODUCTION

Data compression has become a major research area for scientists throughout the world with the ever growing use of multimedia in communication, data transmission and data storage. Decades ago, hard copies images were used for data storage and communication purposes but with the advent of computers, digital file formats have replaced the hard copies. Now, internet and fax are mostly used for data transmission and communication purposes. Images contain significant details, both necessary and redundant. Redundancies are present in co-related data. There are some places like government and private offices, websites where millions of images are stored for records. If these images are stored in their uncompressed form, they may cause huge financial burden on the organization as they need costly communication channels, expensive hardware for required storage and higher bandwidth

Computer-Aided Design & Applications, 9(4), 2012, 531-547

© 2012 CAD Solutions, LLC, <http://www.cadanda.com>

for transmission. Libraries are known to store a large number of books which contain vital information. Many of the books contain important images. Images are damaged overtime due to deterioration of paper in old archives. There is a need to restore these damaged images in their original form. Thus accurate reconstruction of damaged images is an important job in digitizing these libraries.

The objective of image compression is to exclude as much spatial redundancy as possible while retaining necessary details in the reconstructed image. Image compression maybe classified into lossless image compression and lossy image compression. Exact original data can be reconstructed using the algorithms of lossless data compression. In 1980, Knowlton, K. et al. presented a paper on **Progressive transmission of grey scale and binary pictures by simple, efficient, and lossless encoding scheme** [10], Howard P. G. and Vitter J. S. [8] suggested method of lossless image compression using Huffman and arithmetic coding. Lossy image compression is a method of data encoding which achieves compression by discarding some of the data from the image.

There are various methods of lossy image compression like discrete cosine transform (DCT) [1] or wavelet transform and chroma subsampling [24]. In this paper, we have proposed a method for removal of data from images and restoration of images using B-Spline interpolation of gray intensities. A small part of data from the original image is retained and most of it is discarded by data removal method. We have used uniform removal of data in this research. For regenerating an image, pixel intensities (gray values) of the missing points from the image are approximated using third degree B-Spline interpolation. In this manner, images are regenerated from different percentages of data from the original image (image from which data has been removed). The regenerated images are first compared by qualitative analysis, then by quantitative analysis. The method has been discussed in detail for grayscale images but the same method can also be applied for color images. The entire process of data removal and then image reconstruction can be used as a substitute to data compression because good images can be reconstructed from as small as 2% data from the original image. The algorithm of image reconstruction can be also applied to restore deteriorated images and images of inferior quality.

B-Splines have mathematical properties which are advantageous for numerical work, thus they have been used in approximation problems like surface fitting, curve design and interpolation [13]. In 1991, M. Unser et al. [19] presented a paper entitled **Fast B-Splines transforms for continuous image representation and interpolation**. They proved that B-Spline interpolation does not result in loss of resolution of the image and that increasing the order of the spline improves interpolation quality. Thomas M. Lehmann et al. [11] concluded that C^2 continuous cubics were superior to other cubic curves and that B-Spline produced one of the best results in terms of similarity to the original image and it seemed to run faster.

2 DATA REMOVAL

The main advantage of data removal is reduction in file size. Thus it becomes possible to store large number of files in available storage and the transmission of this data becomes economical. We have used uniform removal of data for sampling but data removal can also be non-uniform. We have discussed percentage of data removal in terms of pixels. In this process $(100 - x)$ % of data from the original image is removed and the remaining x % of data is used for image reconstruction as discussed in the procedure of image reconstruction.

2.1 Flowchart for Data Removal Process

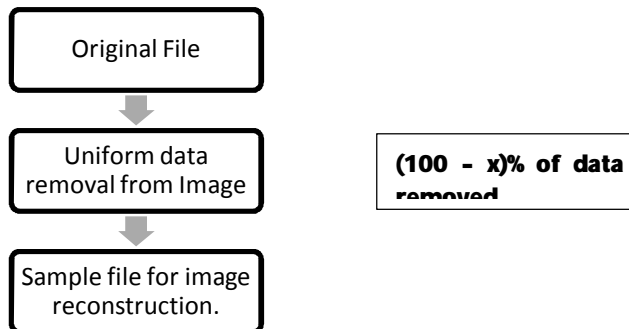


Fig. 1: Flowchart showing data removal process.

2.2 Data Removal Algorithm

Let $B(b_1, b_2, b_3 \dots b_n)$ be the set of pixels from the original image that are to be used for image reconstruction

Let I be the grayscale value at $S(x, y)$

- $S = (x, y, I)$ Point on the image
- Initially $B = \emptyset$ and increment A is known
- Loop1 increment A in x direction
 - Loop2 increment in y direction
 - Add $S(x, y, I)$ to matrix B
 - Endloop2
- Endloop1

Output: Matrix B

Matrix B is the image with removed data. This is used for image reconstruction.

Value of increment A	Percentage of data in matrix B as compared to original Image S (% Pixels)	Compression Ratio (Pixels)
1	100%	1:1
2	25%	4:1
3	11.11%	9:1
4	6.25%	16:1
5	4%	25:1
6	2.78%	36:1
7	2.041%	49:1
8	1.5625%	64:1
9	1.235%	81:1

10	1%	100:1
11	0.826%	121:1
12	0.695%	144:1

Tab. 1: Percentage of data and compression ratio according to value of increment (A).

3 REPRESENTATION OF IMAGE AS A B-SPLINE SURFACE

The image is represented as a B-Spline surface and the pixel intensities are calculated by B-Spline based interpolation. The concept of B-Spline can be extended to represent the pixel intensity on the surface of regenerated surface by introducing a new vector.

$$P = \{x, y, I\}^T; \quad [u, v] \in [0, 1]$$

Here all elements x, y and I are functions of (u, v). I represents the pixel intensity of the points that lie on the surface. The pixel intensities are normalized between 0 and 1 for the purpose of ease of operation.

The B-Spline surface can be represented as follows:

Suppose a set of m+1 and n+1 control points in the u and v direction respectively are given. Order of the B-Spline is p in the u direction and q in the v direction. A point p on the surface of the image is represented by B-Spline as

$$I(u, v) = \sum_{i=0}^m \sum_{j=0}^n N_{i,p}(u) N_{j,q}(v) P_{i,j} \tag{1}$$

Where $P_{i,j} = \{x_{i,j}, y_{i,j}, I_{i,j}\}^T$ are the control points for the B-Spline surface.

The B-Spline basis functions $N_{i,p}$ are as defined recursively [13].

There are different types of knot vectors like open, open uniform and non-uniform. In this case, we have used clamped knot vectors. In clamped knot vectors, the first knot and the last knot must be of the multiplicity p+1, where p is the order of the curve.

Technique A:

In this technique of B-Spline interpolation (also known as B-Spline fit), the surface actually passes through the data points. It is said to fit the data points. Steps for finding the control points are mentioned below.

Let $A = [u, v]^T$ be the set of known data points. These are the points on the image.

Thus,

$$I(u, v) = \sum_{i=0}^m \sum_{j=0}^n N_{i,p}(u) N_{j,q}(v) P_{i,j}$$

The above equation can be represented as

$$[A] = [N] [P]$$

Where

$$N_{i,j} = N_{i,p}(u) N_{j,q}(v)$$

If the matrix N is a square matrix,

$$[P] = [N]^{-1}[A] \quad (2)$$

According to Rogers et al. [15], for non-square matrix N

$$[P] = [[N]^T[N]]^{-1}[N]^T[A] \quad (3)$$

The control points can be found using the above equations which consist of three components, two geometrics (x, y) and the third is the grayscale value (intensity) I at that coordinate (x, y). Now, the equation of B-Spline surface (equation 1) is used to regenerate the image.

For computing inverse of a matrix, Singular value decomposition (SVD) method is generally advised since it has the advantage of being more robust to numerical errors. This approach is computationally expensive to solve when matrices are large [12]. Thus we have used equation (3) for non-square matrices.

Technique B:

In technique B, data points act as the control points and the curve approximates the data points. The equation of a B-Spline surface can be represented as shown in the equation (1).

Code for Reconstruction of Image using technique-B of B-Spline Interpolation from Grayscale Images

```

readImage_data, gray intensities of pixels
KnotVect = fn_KnotVect (order_of_curve, no_of_controlpt)
Loop1 increment u_parameter
  Loop2 increment v_parameter
    Loop3 increment controlpt_u_direction
      Blending_fun1=fn_B_Spline(controlpt_u_direction, order_of_curve, u, KnotVect_u)
      Loop4 increment controlpt_v_direction
        Blending_fun2=fn_B_Spline(controlpt_u_direction, order_of_curve, u, KnotVect_u)
        Image_pixel=fn_bsurf_pt(Blending_fun1, Blending_fun2)
      Endloop4
    Endloop3
  Endloop2
Endloop1

```

3.1 Image Reconstruction Procedure

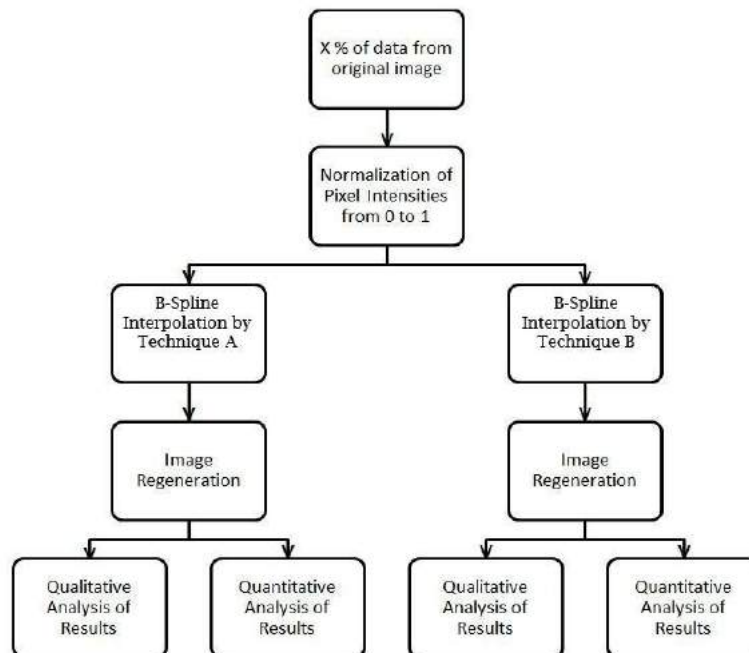


Fig. 2: Flowchart for model regeneration procedure and analysis of results.

3.2 Discussion

The procedure mentioned in the Fig. 2 is applied to different percentages of input data from the original image. Four such results have first been qualitatively analyzed through visual interpretation and then quantitatively compared through error profiles. For better understanding, we have compared results for three different images. Two of the images have distinct boundaries while the third image has indistinct boundaries.

3.2.1 Sample images



Fig. 3: From left to right (a) Image 1 (671x907 pixels) (b) Image 2 (753x653 pixels) (c) Image 3 (410x555 pixels) (d) Image 4 (671x907 pixels).

The first three images are grayscale images and fourth image is colored.

Results of data removal

If Fig. 4 (a) represents the pixels of the sample image, the image formed after data removal algorithm is represented by Fig. 4 (b). Each pixel corresponds to one square block. In Fig. 4 (a), black colored pixel represents the original pixel intensities of corresponding points.

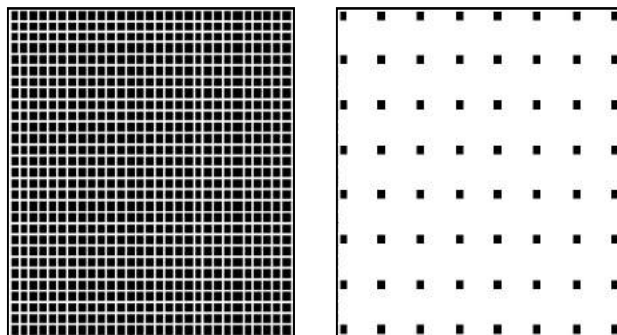


Fig. 4: (a) Source Image S (29x29 pixels) (b) Image showing output of data removal algorithm with increment parameter $A=4$. Removed pixels are shown in white. The unremoved pixels (in original intensity) are tagged with their components $[x, y, I]$ which are used for interpolation

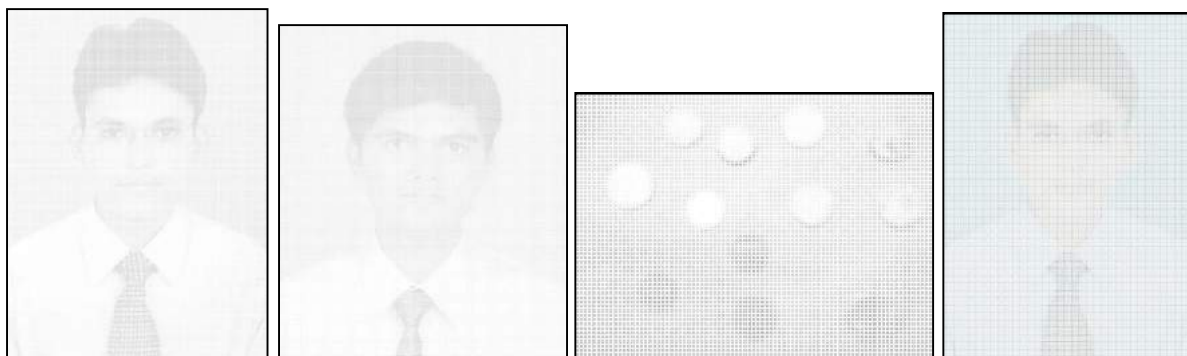


Fig. 5: Images with removed data for: (a) Image 1, (b) Image 2 (c) Image 3 and (d) colored Image 4. The images are showing 11.11% of the original data.

Fig. 5 shows the images with 11.11% of data from sample images. As more data is removed from a sample image, the visibility of the image reduces due to the absence of pixels which were removed during data removal process. Images with data as low as 2% are nearly invisible, thus we have shown the results of data removal algorithm for 11.11% data only (Fig. 5). We have achieved acceptable results for the images reconstructed from less than 2% of data (Tab. 3).

3.2.2 Qualitative analysis

The images regenerated from different percentage of data from original image have been shown in Tab. 3. In general, images regenerated from technique B appear to have smooth boundaries and noticeable blur while the images regenerated from Technique A seem to be more effective in retaining

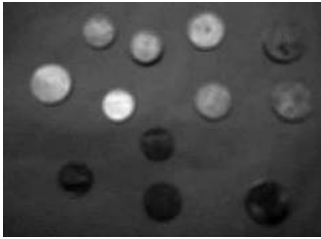
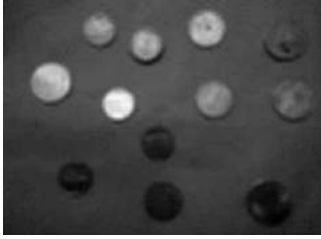
small features but they display significant amount of noise near object boundaries. It can be concluded that technique B produces visually substandard results for images with small percentage of input data (Col I, Tab. 3). Thus, for other images (images 2 and 3) our analysis has been limited to technique A only.

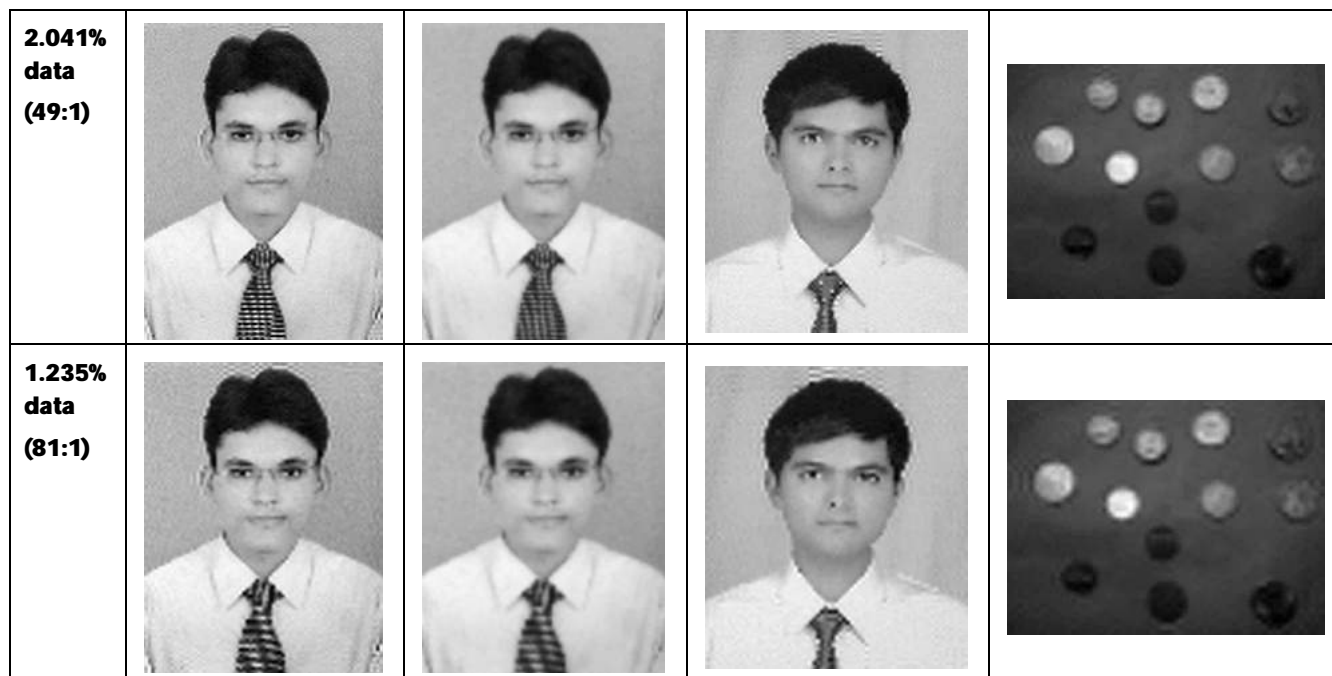
The quality of regenerated images has been correlated to the percentage of data input in Tab. 2.

Percentage of Input data	Regenerated image quality
11.11%	Indistinguishable
4%	Very good
2%	Good
1.235%	Fair

Tab. 2: Quality of regenerated images.

Reconstructed Images

% data / CR	Image 1		Image 2 Technique A	Image 3 Technique A
	Technique A	Technique B		
11.11% data (9:1)				
4% data (25:1)				



Tab. 3: From left to right. Images reconstructed using: (a) technique A and technique B from sampled image1 (b) technique A from sampled image 2 and (c) technique A from sampled image 3 for different percentage of input data.

3.2.3 Quantitative analysis

Quantitative analysis of the regenerated images is done by comparing results on the basis of various parameters like mean error, standard deviation, variance and file size of the regenerated image. Error with respect to above parameters is represented in the graphical form.

3.2.3.1 Surface error profiles

A two dimensional surface error profile is generated by subtracting pixel intensities of regenerated image from pixel intensities of corresponding points on the original image. Magnitude of percentage error at a particular point can be obtained by mapping the color at that point with color bar adjacent to the profile. This profile displays absolute error, that is, it displays only the magnitude of error. Thus information regarding positive or negative nature of the error is missing. Surface error profiles of image 1 for various percentages of input data have been shown in Fig. 6.

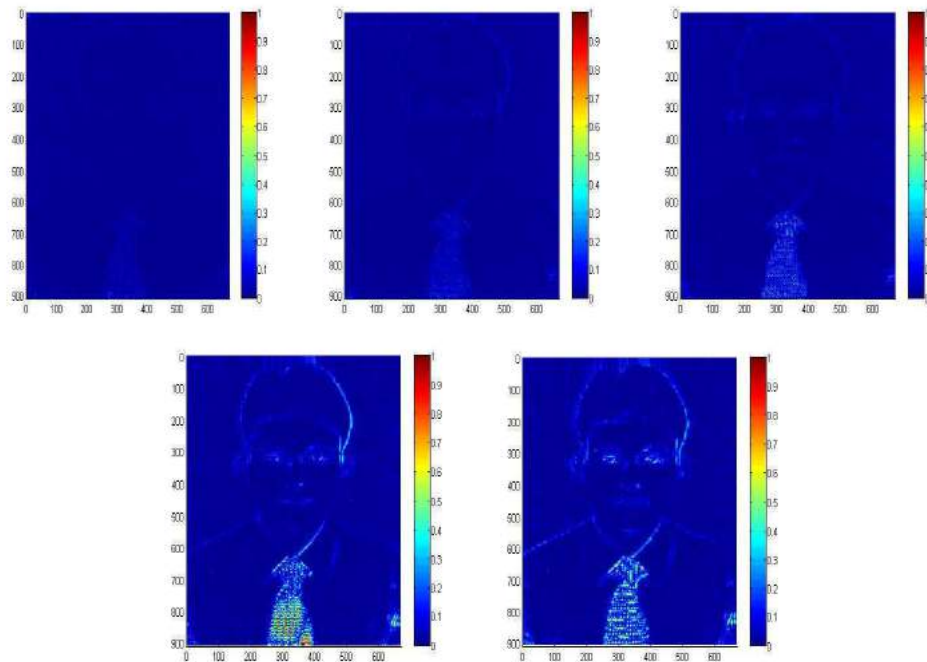


Fig. 6: From left to right and top to bottom: Surface Error Profiles for images regenerated by Technique A using (a) 25%, (b) 11.11%, (c) 4%, (d) 2.041% and (e) 1.235% of input data from Image 1.

3.2.3.2 Peak error profiles

In this error profile, the magnitude of error is calculated in similar manner as the surface error profile. The calculated error is displayed on an analytical 4 dimensional error plot in which magnitude of percentage error is measured along the Z axis and fourth dimension is color. This profile results in much better understanding of magnitude of error at various points on the regenerated image because of the added benefits of better visualization. Another advantage is that this profile displays both, positive and negative error. Error plots above the image surface show positive error at those points while those below the image surface show negative error. Peak error profiles of image 1 reconstructed by Technique A for various percentages of input data have been shown in Fig. 7.

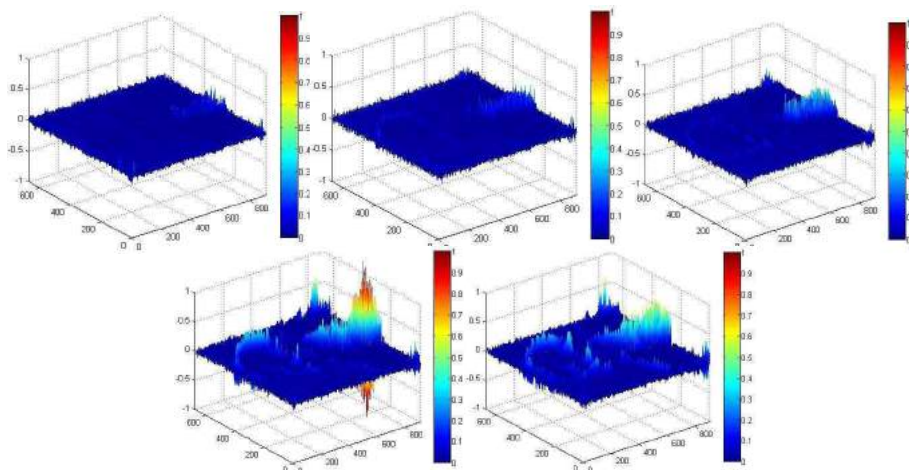


Fig. 7: From left to right and top to bottom: Peak error profiles for images regenerated by Technique A using (a) 25%, (b) 11.11%, (c) 4%, (d) 2.041% and (e) 1.235% of input data from Image 1.

3.2.3.3 Comparison between results produced by techniques A and B

The performance of techniques A and B for image regeneration is quantitatively compared by plotting mean error, standard deviation of errors and variance of errors against the percentage of data input from the original image. Graphs for images 1, 2 and 3 have been shown in figures 8, 9 and 10 respectively.

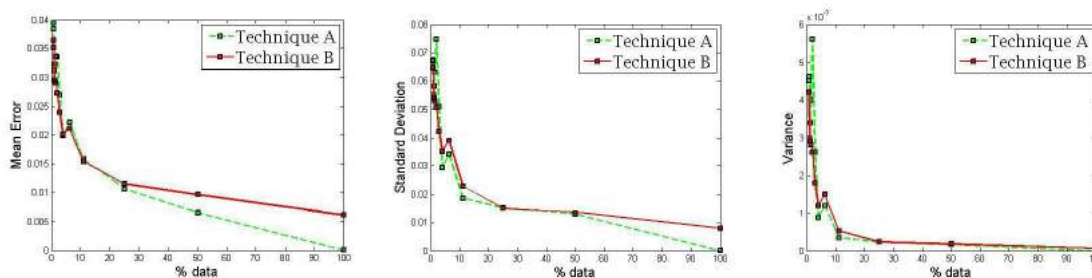


Fig. 8: From left to right. (a) Mean error, (b) Standard deviation of error and (c) Variance of error for techniques A and B of image regeneration against percentage of data input from image 1.

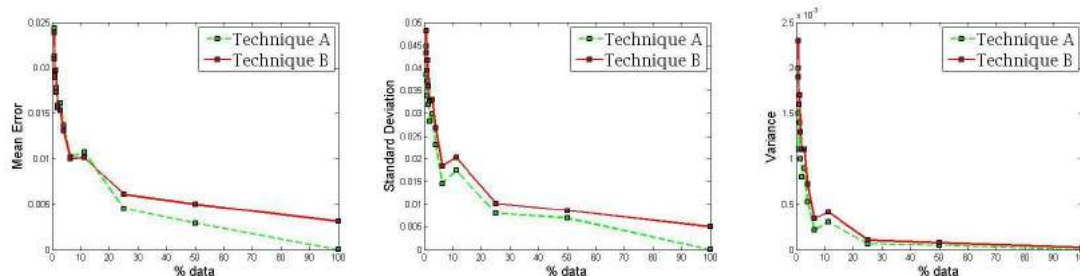


Fig. 9: From left to right. (a) Mean error, (b) Standard deviation of error and (c) Variance of error for techniques A and B of image regeneration against percentage of data input from image 2.

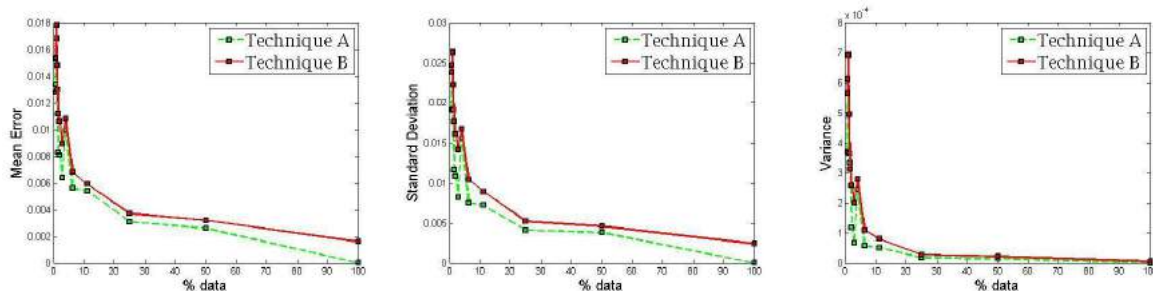


Fig. 10: From left to right. (a) Mean error, (b) Standard deviation of error and (c) Variance of error for techniques A and B of image regeneration against percentage of data input from image 3.

The plots for all the images are in accordance with each other. The respective profiles of the three images are similar. When image is regenerated from 100% data, interpolation using technique A gives zero error while technique B gives some error since the very beginning. We can see that error is relatively smaller in technique A for regeneration of image from 100% to 8% of original data. The error rises slowly from 100% to about 25% of data input, it increases at a higher rate from 25% to about 6% of input data. Then the error rises at a very high rate from 6% to 1% of data input. The magnitude of error in technique A and technique B is almost same for 5% to 1% of data input.

Percentage Data	Image 1 (KB)	Image 2 (KB)	Image 3 (KB)
100 %	211	149	45.1
50 %	134	95.5	27.3
25 %	77.3	59.7	17.4
11.11 %	36.5	29.8	9.66
6.25 %	22.2	18.2	6.21
4 %	14.8	12.2	4.56
2.78 %	10.7	8.96	3.58
2.041 %	8.42	7.04	2.85
1.5625 %	7.23	5.75	2.53
1.235 %	5.80	4.68	2.14
1 %	4.92	4.14	1.78
0.826 %	4.18	3.53	1.72
0.695 %	3.56	2.95	1.53

Tab. 4: From left to right. File size of grayscale images after data removal for: (a) Image 1, (b) Image 2 and (c) Image 3 using different percentages of input data.

3.3 Color Images

Color images can also be regenerated using the above algorithm. The only difference is that the individual R, G and B components of the image have to be removed and then interpolated separately before regeneration of the image. The colored image 4 after data removal process has been shown in

Fig. 5 (d). Images with smaller percentage of input data have not been shown due to poor visibility after data removal. The images regenerated from different percentage of data from original image using both, techniques A and B have been shown below.

Image 4

% data / CR	Technique A	Technique B
11.11% data (9:1)		
4% data (25:1)		
2.78% data (36:1)		



Tab. 5: From left to right. Comparison of color images regenerated from sampled image 4 using: (a) Technique A and (b) Technique B of B-Spline interpolation for different percentage of input data.

It can be observed that interpolation using technique A regenerates better colored images as compared to technique B. The quality of regenerated images has been compared with the percentage of input data in Tab. 6.

Percentage of Input Data	Regenerated Image Quality
11.11%	Indistinguishable
4%	Excellent
2.78%	Very good
2%	Good

Tab. 6: Quality of regenerated colored images.

4 COMPARISON WITH OTHER COMPRESSION TECHNIQUES

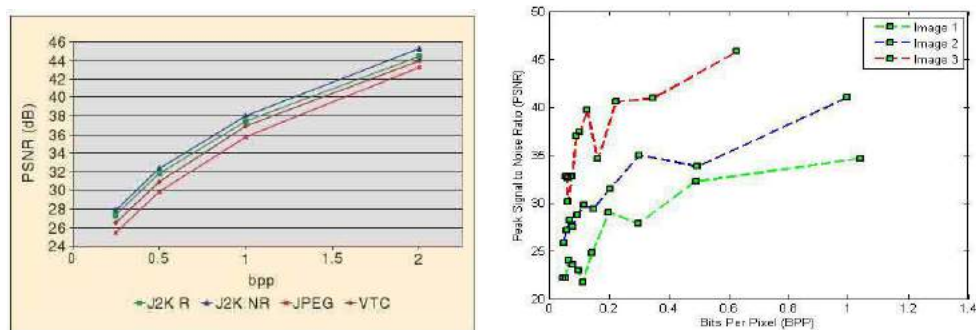


Fig. 11: Left to right. PSNR (dB) vs. bpp graph for: (a) different compression standards, by Skodras, A. et al. [16]. (b) Images 1, 2 and 3 regenerated using Technique A.

Peak Signal to Noise Ratio (PSNR) is used to compare the quality of images regenerated by lossy compression methods. The PSNR results for various compression standards obtained by Skodras, A. et al. [16] has been shown in the Fig. 11 (a) above. The plot of Peak Signal to Noise Ratio (PSNR) against Bits Per Pixel (bpp) for grayscale images reconstructed through B-Splines for images 1, 2 and 3 has been shown in Fig. 11 (b).

Percentage data	Compression ratio	Image 1		Image 2		Image 3	
		bpp	PSNR (dB)	bpp	PSNR (dB)	bpp	PSNR (dB)
25%	4:1	0.994	34.628	1.040	40.969	0.626	45.831
11.11%	9:1	0.496	32.232	0.491	33.788	0.347	40.946
6.25%	16:1	0.303	27.820	0.298	34.988	0.223	40.533
4%	25:1	0.203	29.021	0.199	31.440	0.164	34.641
2.78%	36:1	0.149	24.787	0.144	29.367	0.128	39.663
2.041%	49:1	0.117	21.730	0.113	29.764	0.102	37.391
1.5625%	64:1	0.095	22.920	0.097	28.742	0.091	36.943
1.235%	81:1	0.078	23.549	0.078	27.528	0.077	32.737
1%	100:1	0.069	23.961	0.066	28.215	0.064	30.106
0.826	121:1	0.058	22.190	0.056	27.142	0.061	32.603
0.695	144:1	0.049	22.182	0.047	25.849	0.055	32.738

Tab. 7: From left to right. (a) Percentage data, (b) Compression ratios, (c) bpp and (d) PSNR (dB) values for Images 1, 2 and 3.

5 CONCLUSION

In this paper, methodology was first explained to remove data uniformly from an image and then reconstruction of images from different percentage of input data was successively achieved. Images were regenerated using two different methods of B-Spline interpolation, techniques A and B. Their relative performance was compared using qualitative and quantitative methods. If we visually compare images regenerated by techniques A and B, technique A seems to be more effective in preserving details of small features like eyes and nose from images 1 and 2 but there is significant amount of noise near the edges. Technique B regenerates images with smooth boundary but the images are slightly blurred at high compression ratios. This is because B-Spline surface in technique A passes through all the data points while B-Spline surface in technique B approximates the data points.

The results of quantitative analysis prove that technique A produced superior results as compared to technique B for small compression ratios. The magnitude of error was represented using surface error plots and peak error plots. With the help of these plots, it can be concluded that the error is almost negligible where there is uniform distribution of pixel intensities like the interior of object or the background of the image, significant error exists at the object boundaries and the magnitude of error is maximum at smaller features like the eyes and the tie on images 1 and 2. Another important

observation from the error plots was that the magnitude of error was significantly smaller in image 3 where boundary is slightly blurred and there is a small variation in pixel intensities between the object (coins) and the background. Mean error, standard deviation of error and variance of error were found to be 0.0081, 0.0108 and 1.17×10^{-6} respectively for image 3, while they were 0.0335, 0.0748 and 0.0056 respectively for image 1 when both the images were regenerated from 2% of original data using technique A. Thus it can be concluded that the magnitude of error is large if image regeneration is done from images that have distinct object boundaries. For very-low-quality purposes such as previews or archive indexes images can be slightly blurred and then regenerated to reduce error using B-Splines. The above procedure is equally effective for regenerating color images as shown in Tab. 5. This algorithm enables the data to be stored with lesser disk space (Tab. 4) and reconstruct the images with fairly good results.

6 REFERENCES

- [1] Abe, Y.; Iiguni, Y.: Image restoration from a down sampled image by using the DCT. Signal Processing, 87(10), 2007, 2370-2380. [doi:10.1016/j.sigpro.2007.03.010](https://doi.org/10.1016/j.sigpro.2007.03.010)
- [2] Alirezaie, J.; Jernigan, M.E.: Medical image compression using B-Spline wavelet transform, Engineering in Medicine and Biology Society, IEEE 17th Annual Conference, vol. 1, 1995, 431-432.
- [3] Chong, Michael M.S.; Gay, Robert K.L.; Tan, H.N.; Liu, J.: Automatic representation of fingerprints for data compression by B-Spline functions, Pattern Recognition, 25(10), October 1992, 1199-1210. [doi:10.1016/0031-3203\(92\)90021-A](https://doi.org/10.1016/0031-3203(92)90021-A)
- [4] Fahmy, G.; Aach, T.: Enhanced B-Spline Based Compression Performance for Images, IEEE International Conference on Acoustics, Speech, and Signal Processing (ICASSP), 2010, 1390-1393.
- [5] Fahmy, M.F.; Abdel Raheem, G.M.; Mohammed, U.S.; Fahmy, O.E.: A B-Spline Based Image Compression and Watermarking Technique, IEEE International Symposium on Signal Processing and Information Technology, 2007, 181-184. [doi:10.1109/ISSPIT.2007.4458070](https://doi.org/10.1109/ISSPIT.2007.4458070)
- [6] Howard, P. G.; Vitter, J. S.: Error Modeling for Hierarchical Lossless Image Compression, Proceedings of the 1992 IEEE Data Compression Conference (DCC '92), Snowbird, UT, March 1992 269-278.
- [7] Howard, P. G.; Vitter, J. S.: Fast and efficient lossless image compression, Proc. Of Data Compression Conference, 1993, 351-360.
- [8] Howard, P. G.; Vitter, J. S.: Parallel lossless image compression using Huffman and arithmetic coding, Proc. Data Compression Conference DCC-92, Snowbird, Utah, 1992, 299-308.
- [9] Karczewicz, M.; Gabbouj, M.: ECG data compression by spline approximation, Signal Processing, 59(1), May 1997, 43-59. [doi:10.1016/S0165-1684\(97\)00037-6](https://doi.org/10.1016/S0165-1684(97)00037-6)
- [10] Knowlton, K.: Progressive transmission of grey scale and binary pictures by simple, efficient, and lossless encoding scheme, Proc. IEEE, 1980, 68, 885-896. [doi:10.1109/PROC.1980.11754](https://doi.org/10.1109/PROC.1980.11754)
- [11] Lehmann, T. M.; Gönner, C.; Spitze, K.: Survey: Interpolation Methods in Medical Image Processing, IEEE Transactions On Medical Imaging, 18(11), November 1999, 1049. [doi:10.1109/42.816070](https://doi.org/10.1109/42.816070) PMID:10661324
- [12] Ma, S.; Goldfarb, D.; Chen, L.: Fixed point and Bregman iterative methods for matrix rank minimization, Technical report (2008).
- [13] Mortenson, M. E.: Geometric Modeling, John Wiley & Sons, New York, 1985.
- [14] Pennebaker, W. B.; Mitchell, J. L.: The JPEG Still Image Compression Standard, Kluwer Academic Publishers Norwell, MA, USA, 1992.
- [15] Rogers, D.F.; Adams, J. A.: Mathematical Elements for Computer Graphics, Second Edition, McGraw-Hill, 1976.

- [16] Skodras, A.; Christopoulos, C.; Ebrahimi, T.: The JPEG 2000 Still Image Compression Standard, IEEE Signal Processing Magazine, September 2001, 36 1 58.
- [17] Toraichi, K.; Yang, S.; Kamada, M.; Mo, R.: Two-Dimensional Spline Interpolation for Image Reconstruction, Pattern Recognition, 21(3), 1988, 275-284. [doi:10.1016/0031-3203\(88\)90062-3](https://doi.org/10.1016/0031-3203(88)90062-3)
- [18] Truong, T.K.; Wang, L.J.; Reed, I.S.; Hsieh, W.S.: Image Data Compression Using Cubic Convolution Spline Interpolation, IEEE Transactions On Image Processing, 9(11), November 2000, 1988-1995. [doi:10.1109/83.877222](https://doi.org/10.1109/83.877222) PMID:18262936
- [19] Unser, M.; Aldroubi, A.; Eden M.: Fast B-Spline Transforms for Continuous Image Representation and Interpolation, IEEE Transactions on Pattern Analysis and Machine Intelligence, 13(3), March 1991, 277-285. [doi:10.1109/34.75515](https://doi.org/10.1109/34.75515)
- [20] Van Voorhis, D.: An extended run-length encoder and decoder for compression of black/white images, IEEE Transactions on Information Theory, 22(2), Mar 1976, 190. [doi:10.1109/TIT.1976.1055536](https://doi.org/10.1109/TIT.1976.1055536)
- [21] Wang, L.; Goldberg, M.: Progressive image transmission by multistage transform coefficient quantization, Proc. IEEE Int. Conf. on Communications, Toronto, Ont., June 1986, 419-423
- [22] Wang, L.; Goldberg, M.: Progressive image transmission by transform coefficient residual error quantization, IEEE Trans. Commun. 36(1), 1988, 75-87. [doi:10.1109/26.2731](https://doi.org/10.1109/26.2731)
- [23] Warkhedkar, R. M.; Bhatt, A. D.: Material-solid modeling of human body: A heterogeneous B-Spline based approach, Computer-Aided Design, 41(8), August 2009, 586-597. [doi:10.1016/j.cad.2008.10.016](https://doi.org/10.1016/j.cad.2008.10.016)
- [24] Wong, A.; Bishop, W.: Practical Content-Adaptive Subsampling for Image And Video Compression, Proceedings of the Eighth IEEE International Symposium on Multimedia (ISM'06).
- [25] Yongqing Fu; Fei He; Baosen Song: A New Compression Method of Gray Image, International Conference on Information Engineering and Computer Science (ICIECS), 2009, 1 1 4. [doi:10.1109/ICIECS.2009.5365762](https://doi.org/10.1109/ICIECS.2009.5365762)